# Effects of an environment on a cavity-quantum-electrodynamics system controlled by bichromatic adiabatic passage

H. Eleuch,[1,2] S. Guérin,[3] and H. R. Jauslin[3]

[1]*Institute for Quantum Science and Engineering and Department of Physics and Astronomy, Texas A&M University, College Station, Texas 77843, USA*

[2]*Institut National des Sciences Appliquées et de Technologie Zone Urbaine Nord Tunis, BP 676, Tunis Cedex 1080, Tunisia*

[3]*Laboratoire Interdisciplinaire Carnot de Bourgogne, UMR 6303 CNRS, Université de Bourgogne, BP 47870, F-21078 Dijon, France*

(Received 11 September 2011; published 23 January 2012)

We present a theoretical investigation of a cavity-QED system controlled by bichromatic adiabatic passage in a dissipative environment. We analyze the production of a controlled Fock state in the cavity by a traveling atom simultaneously coupled by a laser field, and the leakage of the corresponding photons from the cavity.

DOI: 10.1103/PhysRevA.85.013830 PACS number(s): 42.50.Pq, 32.80.Qk, 03.65.Yz, 42.50.Ex

## I. INTRODUCTION

The coherent control of photonic states in cavity-QED systems by interfacing it with atoms is of current interest for its potential applications in quantum-information processing [1,2] such as quantum memories and quantum networking [3–5]. This interface between atoms and photons can be realized with atoms that are trapped in the cavity for a sufficiently long time [6–8]. One can alternatively use atoms traveling through the cavity [9,10], which leads to more robust processes for adiabatic dynamics [11].

The adiabatic passage technique is now a widely used tool [12,13]. This technique provides a method for the control of quantum processes by interaction with near-resonant laser pulses that is robust with respect to fluctuations in the parameters as well as to an imperfect knowledge of the system [14]. This technique has been proposed in cavity-QED systems for the purpose of producing quantum gates [15,16] and entanglement [17,18].

Generating one-photon, two-photon, and more generally $n$-photon Fock states in a cavity is another important issue and several techniques have been proposed and tested, based on the control of two-level atoms interacting with a single-mode high-$Q$ cavity and a delayed maser field [9,19–21]. The process can be viewed as the transfer of $n$ photons from a maser field into the cavity, mediated by the atom traveling through the cavity. A method to produce an $n$-photon Fock state in the cavity by bichromatic adiabatic passage (BAP) has been recently proposed [22] in which the specific Fock state is controlled through topological principles. The dynamics of the process can be indeed described in terms of the topology of the dressed eigenenergy surfaces of the atom-laser (or maser)-cavity system where the maser and cavity fields are near resonant with the two-state atom (but of different frequency). This extends the BAP technique with two lasers [23]. The number of exchanged photons depends on the design of the adiabatic dynamics through and around the conical intersections of dressed eigenenergy surfaces. The BAP process was treated as a nondissipative system where the coupling to the environment through atomic spontaneous emission and cavity dissipation was neglected. The goal of this paper is to study the effects of the environment on such cavity-QED systems controlled by a BAP process.

In the next section, we present the model of the atom-maser-cavity system using an effective Hamiltonian based on the Floquet formalism [18]. In Sec. III, we describe the setup for the numerical computation of the time evolution of the density matrix, determined by a Lindblad master equation. In Sec. IV we discuss the different effects of the coupling with the environment on the transfer of population before concluding in Sec. V.

## II. MODEL

The physical situation we consider consists of a high-finesse cavity where a two-level atom (for instance a Rydberg atom) in its lower state goes through a cavity and a laser (or maser) field with velocity $v$ (see Fig. 1). The atom first encounters the vacuum mode of the cavity with frequency $\omega_c$ and waist $W_c$ and then the maser beam with frequency $\omega_L$ and waist $W_L$. Both the laser and the cavity fields are near resonant with the atomic transition. The distance between the crossing points of the cavity and the laser axis with the atomic trajectory is $d$. The traveling atom encounters time-dependent and delayed Rabi frequencies of the cavity and the laser fields of the form

$$G(t) = G_0 e^{-\left(\frac{vt+d/2}{W_c}\right)^2}, \qquad G_0 = -\mu\sqrt{\frac{\omega_c}{2\varepsilon_0 V}}, \tag{1}$$

$$\Omega(t) = \Omega_0 e^{-\left(\frac{vt-d/2}{W_L}\right)^2}, \qquad \Omega_0 = -\mu\epsilon_L, \tag{2}$$

where $\mu$, $V$, and $\epsilon_L$ are, respectively, the atomic dipole moment, the effective volume of the cavity mode, and the amplitude of the laser field; $d$ is the distance between the maxima of the cavity and laser fields. The corresponding delay between the two peaks of the pulses experienced by the atom during its traveling is $\tau_d = d/v$.

The detuning of the laser and cavity fields from the atomic transition frequency $\omega_0$ are denoted by

$$\Delta_c = \omega_0 - \omega_c, \quad \Delta_L = \omega_0 - \omega_L. \tag{3}$$

We take the frequencies of the fields such that their difference is small:

$$\delta \equiv \omega_c - \omega_L = \Delta_L - \Delta_c > 0, \quad \delta \ll \omega_c, \omega_L. \tag{4}$$

We assume that

$$G_0, \Omega_0 \ll \omega_0 \tag{5}$$

 

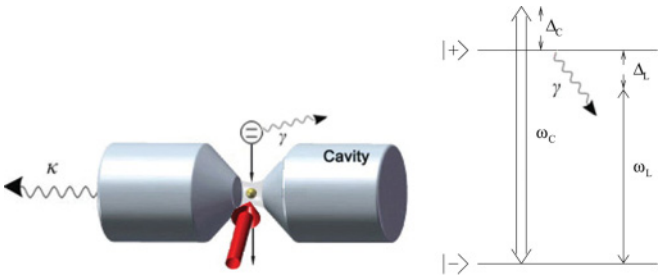


FIG. 1. (Color online) Configuration of the process: A two-level atom travels through a QED cavity and a transverse laser beam. The configuration is such that the cavity and laser fields partially overlap and the cavity field is crossed first by the atom [18].

and, without loss of generality, that $\Omega_0 > 0$, $G_0 > 0$. Under these conditions the reduced effective Hamiltonian obtained from the Floquet theory [13,18] can be written in the following form:

$$\begin{aligned} H_S(t) &= \delta\hbar a^\dagger a + \frac{\hbar}{2}\begin{pmatrix} 2\Delta_M & \Omega(t) \\ \Omega(t) & 0 \end{pmatrix} + \hbar G(t)\begin{pmatrix} 0 & a \\ a^\dagger & 0 \end{pmatrix} \\ &= \delta\hbar a^\dagger a + \hbar\Delta_M D^\dagger D + \frac{\hbar\Omega(t)}{2}(D^\dagger + D) \\ &\quad + \hbar G(t)(aD^\dagger + a^\dagger D), \end{aligned} \tag{6}$$

where the bosonic operator $a$, satisfying $[a,a^\dagger] = 1$, corresponds to the annihilation of one laser photon and creation of one cavity photon, and $D = |-\rangle\langle +|$, $D^\dagger = |+\rangle\langle -|$ are ladder atomic operators, where $|+\rangle$ and $|-\rangle$ represent, respectively, the upper and lower states of the two-level atom.

When the atomic and cavity dissipations are neglected, it was shown in Ref. [18] that it is possible to choose appropriate pulse envelopes which allow the complete adiabatic transfer from the photonic vacuum state and the atomic ground state to a chosen final state, and more specifically to a state formed by the atomic ground state and a chosen Fock state.

In this paper we study the effect of the coupling with the environment. We take into account the atomic spontaneous emission rate $\gamma$ and the cavity dissipation rate $\kappa$. The dynamics of this open system is described by a master equation of the form

$$\frac{d\rho}{dt} = \frac{1}{i\hbar}[H_S,\rho] + \frac{d\rho}{dt}\rfloor_{\text{diss}}, \tag{7}$$

where $\frac{d\rho}{dt}\rfloor_{\text{diss}}$ represents the interaction with the environment modeled by a thermal reservoir. In the Born-Markov approximation the coupling with the environment can be described by a Lindblad equation with a dissipative term of the form

$$\begin{aligned} \frac{d\rho}{dt}\rfloor_{\text{diss}} &= \frac{\gamma}{2}([D\rho,D^\dagger] + [D,\rho D^\dagger]) \\ &\quad + \frac{\kappa}{2}([a\rho,a^\dagger] + [a,\rho a^\dagger]). \end{aligned} \tag{8}$$

In the basis of the bare atom the density operator can be expanded as

$$\rho = \begin{pmatrix} \rho_{++} & \rho_{+-} \\ \rho_{-+} & \rho_{--} \end{pmatrix} \tag{9}$$

with $\rho_{ij} \equiv \langle i|\rho|j\rangle$. The time evolution of the coefficients of this matrix can be derived from the master equation (7):

$$\begin{aligned} \frac{d\rho_{++}}{dt} &= -\left[\left(\frac{\kappa}{2} + i\delta\right)a^\dagger a + \gamma\right]\rho_{++} + \left(i\delta - \frac{\kappa}{2}\right)\rho_{++}a^\dagger a \\ &\quad + \kappa a\rho_{++}a^\dagger - i\frac{\Omega(t)}{2}(\rho_{-+} - \rho_{+-}) \\ &\quad - iG(t)(a\rho_{-+} - \rho_{+-}a^\dagger), \end{aligned} \tag{10}$$

$$\begin{aligned} \frac{d\rho_{+-}}{dt} &= -\left[\left(\frac{\kappa}{2} + i\delta\right)a^\dagger a + \left(\frac{\gamma}{2} + i\Delta_M\right)\right]\rho_{+-} \\ &\quad + \left(i\delta - \frac{\kappa}{2}\right)\rho_{+-}a^\dagger a \\ &\quad + \kappa a\rho_{+-}a^\dagger + i\frac{\Omega(t)}{2}(\rho_{++} - \rho_{--}) \\ &\quad + iG(t)(\rho_{++}a - a\rho_{--}), \end{aligned} \tag{11}$$

$$\begin{aligned} [-22pt]\frac{d\rho_{-+}}{dt} &= -\left[\left(\frac{\kappa}{2} + i\delta\right)a^\dagger a + \left(\frac{\gamma}{2} - i\Delta_M\right)\right]\rho_{-+} \\ &\quad + \left(i\delta - \frac{\kappa}{2}\right)\rho_{-+}a^\dagger a \\ &\quad + \kappa a\rho_{-+}a^\dagger - i\frac{\Omega(t)}{2}(\rho_{++} - \rho_{--}) \\ &\quad - iG(t)(a^\dagger\rho_{++} - \rho_{--}a^\dagger), \end{aligned} \tag{12}$$

$$\begin{aligned} \frac{d\rho_{--}}{dt} &= -\left[\left(\frac{\kappa}{2} + i\delta\right)a^\dagger a + \gamma\right]\rho_{--} + \left(i\delta - \frac{\kappa}{2}\right)\rho_{--}a^\dagger a \\ &\quad + \kappa a\rho_{--}a^\dagger - i\frac{\Omega(t)}{2}(\rho_{+-} - \rho_{-+}) \\ &\quad - iG(t)(a^\dagger\rho_{+-} - \rho_{-+}a). \end{aligned} \tag{13}$$

These equations show that the amplitude of the excitation $\Omega$ and the coupling $G$ link the population evolutions to the coherences.

To solve the master equation numerically, we restrict our computation to a maximum of $N \gg 1$ photons in the cavity using the basis $\{|0\rangle,\ldots,|N\rangle\}$ of the corresponding Fock states. This leads to a Hilbert space of $2(N+1)$ dimensions and to density matrix elements of the form $\rho_{ij,kl}$ with $i,j = \pm$ and $k,l = 0,1,\ldots,N$. We rearrange the $2(N+1)\times 2(N+1)$ elements of the density matrix $\rho$ into a vector $\vec{\rho}(t)$ of $4(N+1)^2$ components, as shown in detail in the next section.

## III. LINDBLAD EQUATION COMPUTATION METHOD

In Refs. [24,25] the master equation of a dissipative multilevel system was solved by transforming the Lindblad equation, which is a matrix differential equation, into a vector differential equation, which is referred to as the Redfield form of the Lindblad equation (or Redfield equation). This method allows a simple numerical computation.

In this section we formulate explicitly this transformation of the matrix differential equation (7) in the space of $2(N+1)\times 2(N+1)$ dimensions into a vector differential equation in the Redfield space $\mathcal{L}$ of $4(N+1)^2$ dimensions in a general and compact form:

$$\frac{d}{dt}\vec{\rho}(t) = \mathbf{L}\vec{\rho}(t), \tag{14}$$

where $\mathbf{L}$ is a matrix and the vector $\vec{\rho}(t)$ is expanded as

$$\vec{\rho}(t) = \begin{bmatrix} \rho_{++00} \\ \rho_{++01} \\ \vdots \\ \rho_{++NN} \\ \rho_{+-00} \\ \vdots \\ \rho_{+-NN} \\ \rho_{-+00} \\ \vdots \\ \rho_{-+NN} \\ \rho_{--00} \\ \vdots \\ \rho_{--NN} \end{bmatrix}. \tag{15}$$

The vector $\vec{\rho}(t)$ can be interpreted as a generalization of the Bloch vector.

We choose a convenient basis $\{B_j\}$, $j = 1, \ldots, 4(N+1)^2$ of matrices of dimension $2(N+1) \times 2(N+1)$ such that

$$(B_j)_{kl} = \begin{cases} 1 & \text{if condition} \quad C_1, \\ 0 & \text{else}, \end{cases} \tag{16}$$

where the condition $C_1$ is defined as

$$C_1 : \begin{cases} 2(N+1)p < j \leqslant 2(N+1)(p+1), \\ k = p+1, \quad l = j - 2(N+1)p, \\ p \in \{0, 1, \ldots, 2N+1\}. \end{cases} \tag{17}$$

This means that the elements of $B_j$ are zero except for one element that has the value 1, whose position is different for the $4(N+1)^2$ matrices. On $\mathcal{L}$ we define a scalar product of two operators $\widetilde{A}$ and $\widetilde{B}$ as

$$(\widetilde{A}, \widetilde{B}) = \mathrm{Tr}(\widetilde{A}^\dagger \widetilde{B}). \tag{18}$$

The basis $\{B_j\}$ is orthonormal with respect to this scalar product.

Any operator $\widetilde{A}$ acting in $\mathcal{L}$ can be represented by the coefficient $a_j$ with respect to this basis:

$$\widetilde{A} = \sum_{j=1}^{4(N+1)^2} a_j B_j, \quad a_j = \mathrm{Tr}(B_j^\dagger \widetilde{A}). \tag{19}$$

In the master equation, we have terms of the form $A\rho$, $\rho C$, and $A\rho C$. We have thus to express in matrix form products of operators, $\widetilde{A}\widetilde{\rho}$, $\widetilde{\rho}\widetilde{C}$, and $\widetilde{A}\widetilde{\rho}\widetilde{C}$, respectively, in $\mathcal{L}$, where $\widetilde{\rho}$, $\widetilde{A}$, and $\widetilde{C}$ are the matrix representation defined by

$$\widetilde{\rho} = \sum_{k=1}^{4(N+1)^2} \rho_k B_k, \quad \widetilde{C} = \sum_{m=1}^{4(N+1)^2} c_m B_m, \tag{20}$$

where the elements $\rho_k$ form the elements of the vector $\vec{\rho}(t)$. We determine the coefficients $(\widetilde{A}\widetilde{\rho})_j$ defined as

$$\widetilde{A}\widetilde{\rho} = \sum_{j=1}^{4(N+1)^2} (\widetilde{A}\widetilde{\rho})_j B_j \tag{21}$$

from (19):

$$(\widetilde{A}\widetilde{\rho})_j = \mathrm{Tr}(B_j^\dagger \widetilde{A}\widetilde{\rho}) = \sum_{k=1}^{4(N+1)^2} \sum_{l=1}^{4(N+1)^2} a_k \rho_l \mathrm{Tr}(B_j^\dagger B_k B_l)$$
$$= \sum_{k=1}^{4(N+1)^2} (\mathbf{L}_A)_{jk} \rho_k, \tag{22}$$

which leads to

$$\overrightarrow{A\rho} = \mathbf{L}_A \vec{\rho}, \quad (\mathbf{L}_A)_{jk} = \sum_{l=1}^{4(N+1)^2} a_l \mathrm{Tr}(B_j^\dagger B_l B_k). \tag{23}$$

With the same procedure, we obtain

$$\overrightarrow{\rho C} = \mathbf{R}_C \vec{\rho}, \quad (\mathbf{R}_C)_{jk} = \sum_{l=1}^{4(N+1)^2} c_l \mathrm{Tr}(B_j^\dagger B_k B_l), \tag{24}$$

and

$$\overrightarrow{A\rho C} = \mathbf{S}_{AC} \vec{\rho}, \quad (\mathbf{S}_{AC})_{jk} = \sum_{l,m=1}^{4(N+1)^2} a_l c_m \mathrm{Tr}(B_j^\dagger B_l B_k B_m). \tag{25}$$

We have thus transformed $\widetilde{A}\widetilde{\rho}$, $\widetilde{\rho}\widetilde{C}$, and $\widetilde{A}\widetilde{\rho}\widetilde{C}$ into, respectively, $\mathbf{L}_A \vec{\rho}(t)$, $\mathbf{R}_C \vec{\rho}(t)$, and $\mathbf{S}_{AC} \vec{\rho}(t)$ in the space $\mathcal{L}$. These expressions are easy to compute numerically in the general case.

## IV. POPULATION TRANSFER AND THE EFFECT OF THE COUPLING WITH THE ENVIRONMENT

In order to study the effect on the population transfer of the coupling with the environment, we determine first the shape of the maser field and cavity coupling adapted to produce one or two photons inside the cavity without atomic and cavity dissipation ($\gamma = \kappa = 0$). The transfer of photons from the maser field into the cavity is based on the adiabatic passage between two dressed states of the coupled atom-maser-cavity system [18]. The method consists of four steps. One starts with the calculation of the dressed energy surfaces of the effective Hamiltonian as functions of the two field amplitudes $\Omega$ and $G$. Then one determines the intersections of the surfaces. They provide the possible paths that can link different states by adiabatic passage. The topology of these surfaces and their intersections gives insight into the various atomic population and photon transfers that can be produced by choosing appropriately the temporal evolution of the pulses. Finally, the adiabatic approximation is applied in order to determine the dynamics of the processes. This method of control is robust because it does not depend on the precise shapes of the fields or on the precise tuning of maser and cavity frequencies.

In what follows, we normalize all time parameters in units of $1/\delta$ (and thus all frequency parameters in units of $\delta$) and the waists in units of $v/\delta$. We consider the detunings such that $\Delta_M = \delta/2$ and using an interaction time $T_{\mathrm{int}}$. Adiabatic passage necessitates $\delta T_{\mathrm{int}} \gg 1$, $\Omega_0 T_{\mathrm{int}} \gg 1$, and $G_0 T_{\mathrm{int}} \gg 1$. Specific ranges of values $\Omega_0$ and $G_0$ (typically of the same order of magnitude as $\delta$) allow the control of the final number of photons in the cavity [18].

We can for instance assume that the atoms go through the cavity with a velocity $v = 100$ m/s and an interaction time

$T_{\rm int} = 100\ \mu$s [26]. We can choose the detuning such that $T_{\rm int} = 100/\delta$ satisfies the condition of global adiabaticity.

### A. Lossless population transfer

We first consider the production of a single-photon state (Fig. 2) and a two-photon state (Fig. 3) in the cavity by adiabatic passage, assuming no loss. The populations of the following figures are determined numerically from the Liouville–von Neumann equation (7). Figures 2(a) and 3(a) represent the time evolution for the two pulses $\Omega$ and $G$, experienced by the atom during its traveling, for one-photon and two-photon transfer, respectively.

The time evolution of the populations $\rho_{00,--}$, $\rho_{11,--}$, and $\rho_{22,--}$, which represent respectively the probabilities of zero, one, and two photons inside the cavity with the atom in the ground state, are plotted in Figs. 2(b) and 3(b) for the lossless case with the initial state of the system: $\rho_{ijkl} = 0$ for all $i$, $j$, $k$, and $l$, except $\rho_{00--} = 1$. Only the most appreciable populations have been plotted. The total expectation probabilities of one photon and two photons in the cavity, respectively $\rho_{ii} = \rho_{--,ii} + \rho_{++,ii}, i = 1,2$, are also plotted in Figs. 2(b) and 3(b). These figures show that the population evolves to a single final state with the atom back

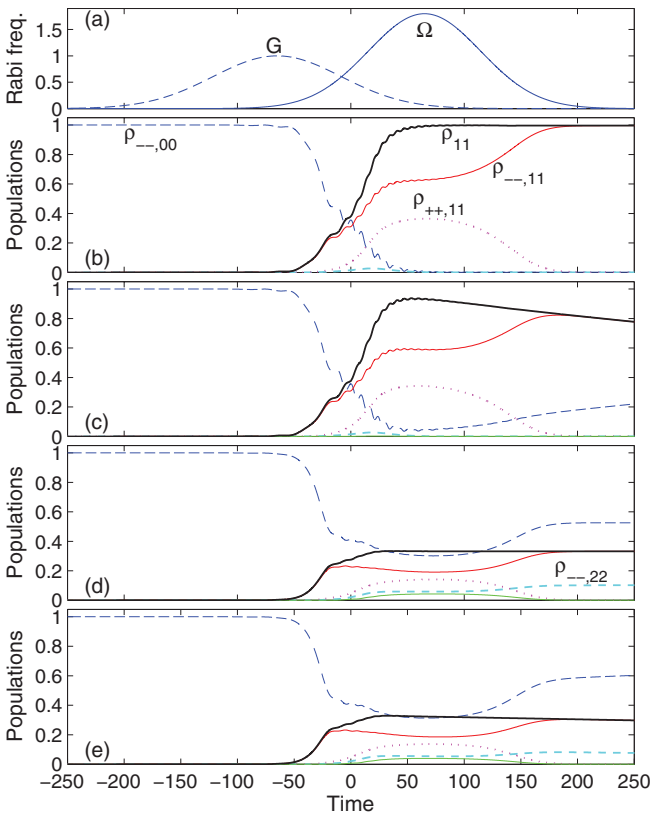


FIG. 2. (Color online) Production of a photon in the cavity: (a) Rabi frequencies (in units of $\delta$) as functions of time (in units of $1/\delta$); (b) corresponding dynamics of the populations for negligible dissipations. The total population of one photon is $\rho_{11} = \rho_{--,11} + \rho_{++,11}$. Dynamics for (c) $\gamma = 0$ and $\kappa = \delta/1000$, (d) $\gamma = \delta/10$ and $\kappa = 0$, and (e) $\gamma = \delta/10$ and $\kappa = \delta/1000$. The other parameters are $\Delta_M = \delta/2$, $W_{at} = 80v/\delta$, $W_c = 70v/\delta$, $\Omega_0 = 1.8\delta$, $G = \delta$, and $d = 130v/\delta$ (i.e., $\tau_d = 130/\delta$).

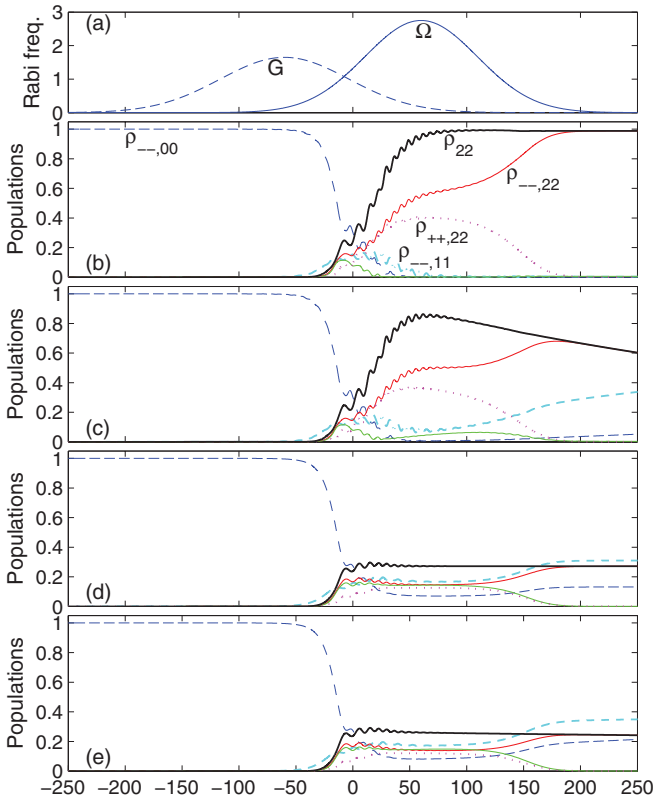


FIG. 3. (Color online) Same as Fig. 2 but for the production of two photons (with $\rho_{22} = \rho_{--,22} + \rho_{++,22}$) in the cavity, and the parameters $\Omega_0 = 2.75\delta$, $G = 1.65\delta$, and $d = 120v/\delta$ (i.e., $\tau_d = 120/\delta$).

in its ground state, with respectively 99.6% probability in the one-photon configuration [Fig. 2(b)] and 98.7% probability in the two-photon configuration [Fig. 3(b)]. These results are close to those of Ref. [18] obtained with different parameters of the fields (Rabi frequencies, waists, and time delay). This confirms the robustness of the adiabatic control method.

### B. The effect of atomic spontaneous emission

In this section we analyze the effect of the atomic spontaneous emission, assuming an ideal cavity. We consider two values of the spontaneous emission corresponding to two atomic systems: circular Rydberg atoms and helium. The radiative lifetime of circular Rydberg states (corresponding to large principal and maximum orbital and magnetic quantum numbers), which is of the order of $T_{at} = 30$ ms (corresponding to $\gamma = \delta/30000$), is much longer than the radiative lifetime of the noncircular Rydberg states. Experimental realization of these states was achieved in Ref. [26] with principal quantum numbers of the order of 50. On the other hand, the radiative lifetime of a helium atom is of the order of 10 $\mu$s (corresponding to $\gamma = \delta/10$).

For the case of the circular Rydberg atoms, the loss $\gamma = \delta/30000$ is very weak since the dynamics obtained for the production of one and two photons is undistinguishable from the lossless dynamics [see Figs. 2(b) and 3(b), respectively].

For the case of helium atoms, the loss $\gamma = \delta/10$ is relatively strong since the dynamics shows a much reduced efficiency for

the targeted production of one and two photons [see Figs. 2(d) and 3(d), respectively]. The final probability of producing one photon (two photons) in the first (second) case is 0.33 (0.27). In the second case, we can notice that the probability to find a single photon is even a bit larger than the one to find a two-photon state. This shows that the population transfer to two-photon states is more sensitive to spontaneous emission than the transfer to single-photon states. This is due to the fact that more energy is needed to produce two-photon states.

### C. The effect of cavity dissipation

We now analyze the effect of the cavity dissipation alone, setting the rate of spontaneous emission to zero. We consider the quality factor of the cavity in a range that corresponds to two recent experimental setups:

(1) In the experiment of Ref. [26] a cavity with $Q = 3 \times 10^8$ was used, corresponding to a photon lifetime inside the cavity of $T_r = 1$ ms and a normalized cavity dissipation rate $\kappa = 1/1000$.

(2) In the experiment of Ref. [27] a cavity with $Q = 4 \times 10^{10}$ was used, with a photon storage time $T_r = 0.3$ s corresponding to a normalized cavity dissipation rate $\kappa = 1/300\,000$.

For the second case ($\kappa = 1/300\,000$), the dissipation does not show a significant effect on the scale of Figs. 2(b) and 3(b). The photons escape from the cavity a long time after the process.

Figures 2(c) and 3(c) display the dynamics for the first case ($\kappa = 1/1000$) for the targeted state of one and two photons, respectively. One can notice that the photons start to escape from the cavity before the process ends. An important issue is the determination of the photon probability outside the cavity. For this study, we consider negligible losses by spontaneous emission, and we assume that the cavity is lossy though the mirror of a single side (see Fig. 1), such that the outgoing photon wave packet travels along the cavity axis in a unique direction. We can calculate the mean number of output photons leaking from the cavity, defined as (see Refs. [28–32])

$$n_{\rm out}(t) = \kappa \int_{-\infty}^{t} \langle a^\dagger(t')a(t')\rangle dt' \tag{26}$$

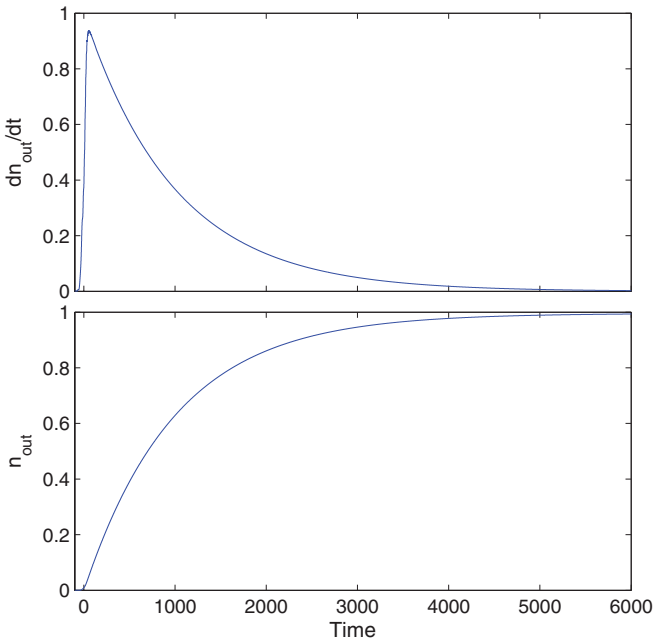


FIG. 4. (Color online) Mean output photon flux (upper frame) and mean output photon number (lower frame) vs time (in units of $1/\delta$) corresponding to the parameters of Fig. 2(c).

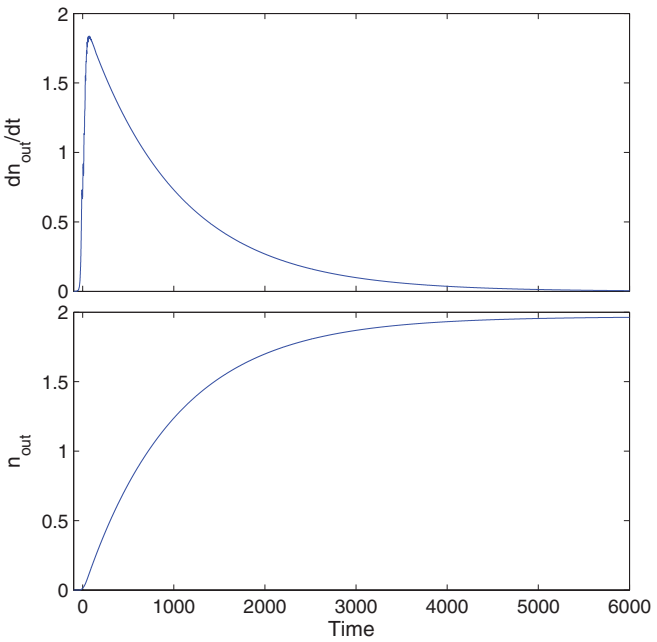


FIG. 5. (Color online) Same as Fig. 4, but corresponding to the parameters of Fig. 3(c).

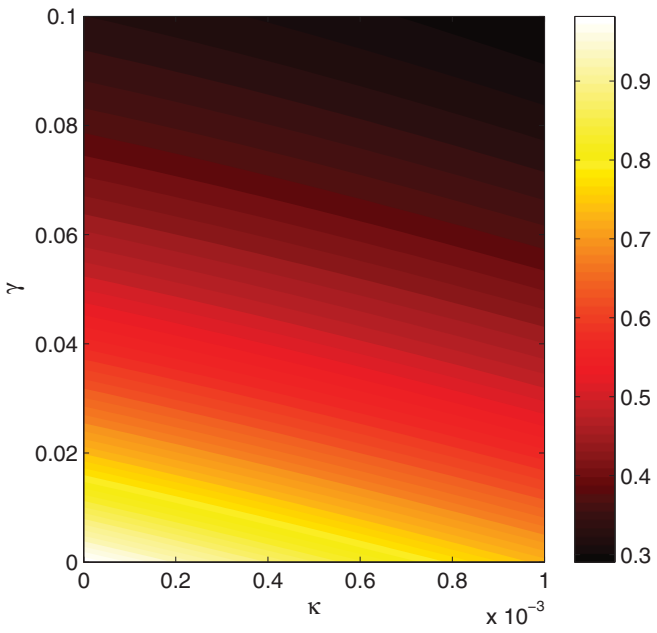


FIG. 6. (Color online) Contour plot of the final population $\rho_{11}$ (at time $t = 300/\delta$) for one-photon transfer as a function of atomic dissipation rate $\gamma$ and cavity dissipation rate $\kappa$ (both in units of $\delta$).

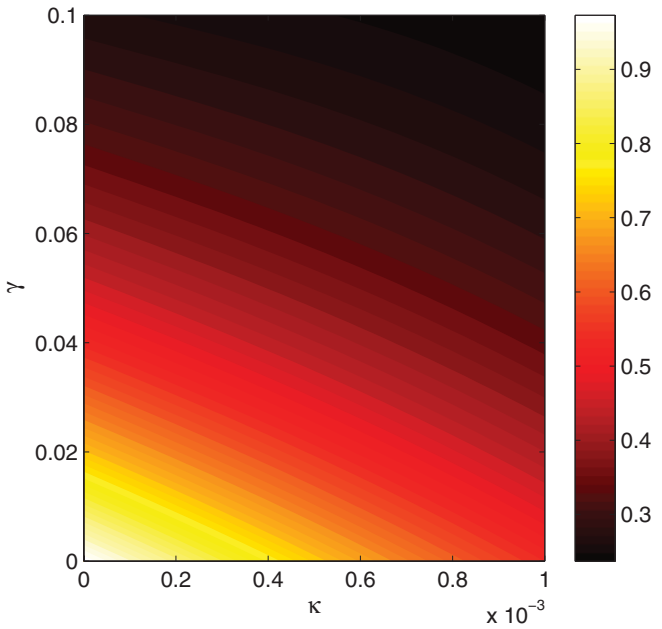


FIG. 7. (Color online) Contour plot of the final population $\rho_{22}$ (at time $t = 300/\delta$) for two-photon transfer as a function of atomic dissipation rate $\gamma$ and cavity dissipation rate $\kappa$ (both in units of $\delta$).

from the flux $dn_{\text{out}}/dt = \kappa\langle a^\dagger(t)a(t)\rangle$ using

$$\langle a^\dagger(t)a(t)\rangle = \text{Tr}[\rho(t)a^\dagger a] = \sum_{n=1}^{N} n(\rho_{++nn} + \rho_{--nn}). \quad (27)$$

Figures 4 and 5 shows the situation when one photon (two photons) is (are) targeted with the parameters of Fig. 2(c) [Fig. 3(c)]. One can notice that, despite the fact that the photon(s) are not fully produced in the cavity before the damping takes place, they are produced outside the cavity with the same probability as they were produced in the cavity without damping. This is well satisfied in both cases for cavity dissipation rates as high as $\kappa \approx \delta/100$.

### D. The effect of cavity and atom dissipations

Figures 6 and 7 display the contour plots of the final photonic population as a function of the joint effects of the cavity and the atomic dissipation rates for one- and two-photon transfers, respectively. Regions with lighter shading correspond to more efficient transfer. These figures show that the transfer is more sensitive to the cavity dissipation than to the atomic spontaneous emission since the spontaneous emission occurs only transiently (when the upper state is populated during the process). One can also notice that the two-photon transfer is globally more sensitive to the dissipations than the one-photon transfer with a more pronounced effect of the cavity dissipation.

Figures 2(e) and 3(e) show an example of dynamics with $\kappa = 1/1000$ and $\gamma = 1/10$; they are very close to the ones of Figs. 2(d) and 3(d), respectively, as the spontaneous emission loss dominates.

## V. CONCLUSION

We have presented a theoretical study of a cavity-QED system controlled by bichromatic adiabatic passage and coupled with an external environment. More precisely, we have investigated the effects of the coupling with an external environment via atomic spontaneous emission and a nonideal cavity. We have studied two situations corresponding respectively to the production of one and two photons in the cavity. We have shown that the photonic population transfer is globally more sensitive to the cavity dissipation. Furthermore, we have demonstrated that the two-photon transfer is more strongly affected by the atomic and cavity dissipations compared to the one-photon transfer.

In the case of relatively large cavity dissipation rate, we have also determined the probability of the output photons leaking from the cavity through a single dissipative mirror, for the one-photon and the two-photon transfers.

The state-of-the-art technology would in principle allow the experimental demonstration of these photonic transfers in the cavity if it featured a sufficiently small dissipation rate and if it is mediated by atoms of weak spontaneous emission. This is the case using maser fields and circular Rydberg atoms.

## ACKNOWLEDGMENTS

We acknowledge the support from the French Agence Nationale de la Recherche (Project CoMoC), the European Marie Curie Initial Training Network Grant No. GA-ITN-214962-FASTQUAST, and from the Conseil Régional de Bourgogne.

[1] M. A. Nielsen and I. L. Chuang, *Quantum Computation and Quantum Information* (Cambridge University Press, Cambridge, UK, 2000).
[2] S. Haroche and J.-M. Raimond, *Exploring the Quantum: Atoms, Cavities and Photons* (Oxford University Press, Oxford, UK, 2006).
[3] J. I. Cirac, P. Zoller, H. J. Kimble, and H. Mabuchi, Phys. Rev. Lett. **78**, 3221 (1997).
[4] H. J. Kimble, Nature (London) **453**, 1023 (2008).
[5] A. Kuhn and D. Ljunggren, Contemp. Phys. **51**, 289 (2010).
[6] M. Keller, B. Lange, K. Hayasaka, W. Lange, and H. Walther, Nature (London) **431**, 1075 (2004).
[7] A. D. Boozer, A. Boca, R. Miller, T. E. Northup, and H. J. Kimble, Phys. Rev. Lett. **98**, 193601 (2007).
[8] H. P. Specht, C. Nölleke, A. Reiserer, M. Uphoff, E. Figueroa, S. Ritter, and G. Rempe, Nature (London) **473**, 190 (2011).
[9] X. Maître, E. Hagley, G. Nogues, C. Wunderlich, P. Goy, M. Brune, J.-M. Raimond, and S. Haroche, Phys. Rev. Lett. **79**, 769 (1997).
[10] H. Walther, B. T. H. Varcoe, B.-G. Englert, and T. Becker, Rep. Prog. Phys. **69**, 1325 (2006).
[11] T. Wilk, S. C. Webster, A. Kuhn, and G. Rempe, Science **317**, 488 (2007).

[12] N. V. Vitanov, M. Fleischhauer, B. W. Shore, and K. Bergmann, Adv. At. Mol. Opt. Phys. **46**, 55 (2001); N. V. Vitanov, T. Halfmann, B. W. Shore, and K. Bergmann, Annu. Rev. Phys. Chem. **52**, 763 (2001).

[13] S. Guérin and H. R. Jauslin, Adv. Chem. Phys. **125**, 147 (2003).

[14] L. P. Yatsenko, S. Guérin, and H. R. Jauslin, Phys. Rev. A **65**, 043407 (2002).

[15] H. Goto and K. Ichimura, Phys. Rev. A **70**, 012305 (2004).

[16] N. Sangouard, X. Lacour, S. Guérin, and H. R. Jauslin, Phys. Rev. A **72**, 062309 (2005); X. Lacour, N. Sangouard, S. Guérin, and H. R. Jauslin, *ibid.* **73**, 042321 (2006).

[17] C. Marr, A. Beige, and G. Rempe, Phys. Rev. A **68**, 033817 (2003).

[18] M. Amniat-Talab, S. Guérin, N. Sangouard, and H.-R. Jauslin, Phys. Rev. A **71**, 023805 (2005); M. Amniat-Talab, S. Guérin, and H.-R. Jauslin, *ibid.* **72**, 012339 (2005).

[19] B. T. H. Varcoe, S. Brattke, M. Weidinger, and H. Walther, Nature (London) **403**, 743 (2000).

[20] P. Domokos, M. Brune, J. M. Raimond, and S. Haroche, Eur. Phys. J. D **1**, 1 (1998).

[21] P. Bertet, S. Osnaghi, P. Milman, A. Auffeves, P. Maioli, M. Brune, J. M. Raimond, and S. Haroche, Phys. Rev. Lett. **88**, 143601 (2002).

[22] M. Amniat-Talab, S. Lagrange, S. Guérin, and H. R. Jauslin, Phys. Rev. A **70**, 013807 (2004).

[23] S. Guérin, L. P. Yatsenko, and H. R. Jauslin, Phys. Rev. A **63**, 031403(R) (2001); Z. Kis, S. Guérin, and H.-R. Jauslin, J. Phys. Conf. Ser. **268**, 012013 (2011).

[24] A. I. Solomon and S. G. Schirmer, in *Group 24: Physical and Mathematical Aspects of Symmetry*, IOP Conf. Proc. No. 173 (Institute of Physics, London, 2003), p. 485.

[25] S. G. Schirmer, T. Zhang, and J. V. Leahy, J. Phys. A **37**, 1389 (2004).

[26] M. Brune, J. M. Raimond, and S. Haroche, Rev. Mod. Phys. **73**, 565 (2001).

[27] S. Brattke, B. T. H. Varcoe, and H. Walther, Phys. Rev. Lett. **86**, 3534 (2001).

[28] C. K. Law and H. J. Kimble, J. Mod. Opt. **44**, 2067 (1997).

[29] G. S. Vasilev, D. Ljunggren, and A. Kuhn, New J. Phys. **12**, 063024 (2010).

[30] A. Gogyan, S. Guérin, H.-R. Jauslin, and Yu. Malakyan, Phys. Rev. A **82**, 023821 (2010).

[31] C. W. Gardiner and P. Zoller, *Quantum Noise* (Springer, Berlin, 2004).

[32] K. J. Blow, R. Loudon, S. J. D. Phoenix, and T. J. Shepherd, Phys. Rev. A **42**, 4102 (1990).